TÜBİTAK

Turk J Elec Eng & Comp Sci, Vol.20, No.1, 2012, © TÜBİTAK
doi:10.3906/elk-1007-624

Mathematical modeling and vertical flight control of a tilt-wing UAV

Kaan Taha ÖNER[1], Ertuğrul ÇETİNSOY[1], Efe SIRIMOĞLU[1], Cevdet HANÇER[1]
Mustafa ÜNEL[1,*], Mahmut Faruk AKŞİT[1], Kayhan GÜLEZ[2], İlyas KANDEMİR[3]
[1] *Faculty of Engineering and Natural Sciences, Sabancı University,*
Orhanlı, Tuzla, 34956, İstanbul-TURKEY
e-mails: {kaanoner,cetinsoy,efesirimoglu,chancer}@su.sabanciuniv.edu,
e-mails: {munel,aksit}@sabanciuniv.edu
[2] *Electrical and Electronics Engineering Faculty, Yıldız Technical University (YTU)*
Barbaros Bul.-Yıldız, 34349, İstanbul-TURKEY
e-mail: gulez@yildiz.edu.tr
[3] *Faculty of Engineering, Gebze Institute of Technology (GYTE),*
Çayırova-Gebze, 41400, Kocaeli-TURKEY
e-mail: kandemir@gyte.edu.tr

Received: 20.07.2010

Abstract

This paper presents a mathematical model and vertical flight control algorithms for a new tilt-wing unmanned aerial vehicle (UAV). The vehicle is capable of vertical take-off and landing (VTOL). Due to its tilt-wing structure, it can also fly horizontally. The mathematical model of the vehicle is obtained using Newton-Euler formulation. A gravity compensated PID controller is designed for altitude control, and three PID controllers are designed for attitude stabilization of the vehicle. Performances of these controllers are found to be quite satisfactory as demonstrated by indoor and outdoor flight experiments.

Key Words: *Tilt-wing, quadrotor, PID, VTOL, hover*

1. Introduction

Unmanned aerial vehicles (UAVs) designed for various missions such as surveillance and exploration of disasters (fire, earthquake, flood, etc.) have been the subject of a growing research interest in the last decade. Airplanes with long flight ranges and helicopters with hovering capabilities constitute the major mobile platforms used in UAV research. Besides these well known platforms, many researchers recently concentrate on the tilt rotor aerial vehicles combining the advantages of horizontal and vertical flights. Because these new vehicles have no conventional design basis, many research groups build their own tilt-rotor vehicles according to the desired

*Corresponding author: Faculty of Engineering and Natural Sciences, Sabancı University, Orhanlı, Tuzla, 34956, İstanbul-TURKEY

technical specifications and objectives. Variations among different designs of such vehicles arise due to practical considerations. Some large scaled examples of those tilt rotor vehicles can be given as Boeing's V22 Osprey [1] and Bell's Eagle Eye [2]. On the other hand, Arizona State University's tilt-wing HARVee [3] and Compigne University's tilt rotor BIROTAN [4] are smaller scaled examples of vehicles with tilting actuators. Boeing's V44 [5] and Chiba University's QTW UAV [6] are some other examples of tilt-rotor and tilt-wing quadrotors respectively.

One of the major issues in the development of such aerial vehicles is control. In order to develop the flight control systems for autonomous aerial vehicles, accurate dynamic models for their flight envelope are needed. The main difficulties in designing stable feedback controllers stem from nonlinearities and couplings exist in the system. Design, modeling and control of autonomous aerial vehicles have become a very challenging research area since 90s and various controllers designed for the VTOL vehicles with quadrotor configurations exist in the literature. Bouabdallah et al. [7] present a PID controller for a simplified model and an LQ controller for a more sophisticated model. PD [8] and quaternion based PD^2 [9] controllers are also used in quadrotor research. The work in [10] shows the result of optimal controllers based on LQR and State Dependent Riccati Equation. In [11], hover flight and trajectory tracking of a four-rotor autonomous flying vehicle are demonstrated using the presented estimation scheme in combination with a linear quadratic regulator (LQR). In [12], Earl and D'Andrea develop an attitude estimation technique by using a decomposition approach. An output feedback controller with estimators and observers is used in [13]. Backstepping control of Madani and Benallegue [14] is an example of recent non-linear control methods applied on quadrotors. In [15], a comparison of two nonlinear controllers based on integral sliding mode and reinforcement learning are presented. Cheviron et al. [16] present a generic nonlinear model for reduced scale UAVs to design a controller. Hably and Merchand [17] have recently proposed a global asymptotic stabilizing controller under bounded inputs. In [18], a minimalist control strategy for fixed wing micro UAVs that provides airspeed, altitude and heading turn rate control by only using two pressure sensors and a single axis rate gyro is presented. The performance of the designed controllers are directly affected by aerodynamics of the vehicles. Huang et al. [19] emphasize the impact of aerodynamic effects at higher speeds and outdoor conditions.

In this paper, a mathematical model and vertical flight control algorithms for a tilt wing UAV (SUAVI: Sabancı University Unmanned Aerial VehIcle) are presented. The vehicle consists of four rotating wings and four rotors, which are mounted on leading edges of each wing. Nonlinear model of the aerial vehicle is derived using Newton-Euler formulation and linearized around hover conditions. A gravity compensated PID controller is designed for altitude control and three classical PID controllers are designed to achieve attitude stabilization. Proposed controllers are verified with indoor and outdoor experiments, and their performance have been found quite satisfactory.

Organization of the paper is as follows: In section 2, a mathematical model of the tilt-wing aerial vehicle is derived using Newton-Euler formulation. In section 3, PID controllers are designed for altitude and attitude stabilization. In section 4, experimental results are presented. Finally, in section 5 the paper is concluded with some remarks and possible future directions are indicated.

2. A mathematical model for the tilt-wing aerial vehicle

The aerial vehicle considered in this work is equipped with four wings that are mounted at the front and at the back of the vehicle, and can be rotated from vertical to horizontal positions. Figure 1 below shows the aerial

vehicle in vertical and horizontal flight modes. With this wing configuration, the vehicle's airframe transforms

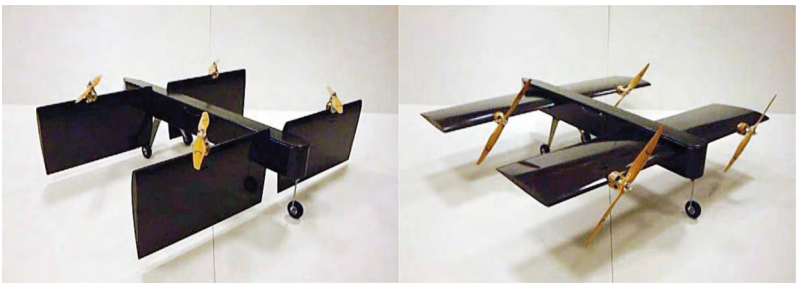

Figure 1. Aerial Vehicle is in vertical (a) and horizontal (b) flight modes.

into a quadrotor structure if the wings are at the vertical position (Figure 1(a)) and into an airplane structure if the wings are at the horizontal position (Figure 1(b)). Two wings at the front can be rotated independently to behave as the ailerons while two wings at the back are rotated together to behave as the elevator. This way the control surfaces of a regular plane in horizontal flight mode are mimicked with minimum number of actuators.

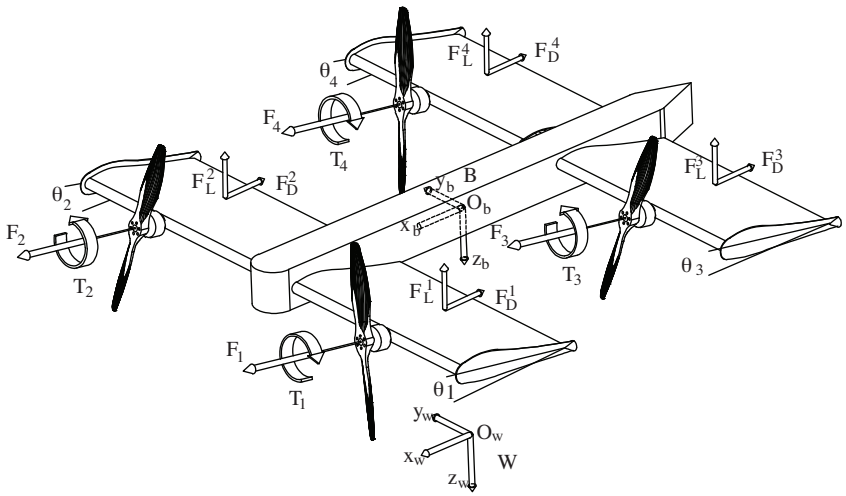

Figure 2. Aerial vehicle in a tilted configuration $(0 < \theta_i < \frac{\pi}{2})$.

The two reference frames given in Figure 2 are body fixed reference frame $B : (O_b, x_b, y_b, z_b)$ and earth fixed inertial reference frame $W : (O_w, x_w, y_w, z_w)$. The position and linear velocity of the vehicle's center of mass in world frame are described as, $P_w = [X, Y, Z]^T$ and $V_w = \dot{P}_w = [\dot{X}, \dot{Y}, \dot{Z}]^T$. The attitude of the vehicle in world frame is given as $\alpha_w = [\phi, \theta, \psi]^T$ where the angular velocity in world frame is given as $\Omega_w = \dot{\alpha}_w = [\dot{\phi}, \dot{\theta}, \dot{\psi}]^T$. In these equations ϕ, θ and ψ are named roll, pitch and yaw angles respectively. The transformation of linear velocities between world and body frames is given as $V_b = [v_x, v_y, v_z]^T = R(\phi, \theta, \psi)V_w$ where the rotation matrix R is defined as $R(\phi, \theta, \psi) = R_z(\psi)R_y(\theta)R_x(\phi)$. The transformation of the angular velocities between world and body frames is given as $\Omega_b = [p, q, r]^T = E(\phi, \theta)\Omega_w$ where the E is the rotational velocity transformation matrix [20].

Using Newton-Euler formulation, the dynamic equations for aerial vehicle in body fixed reference frame B are given as:

$$m\dot{V}_b + \Omega_b \times (mV_b) = F_t, \qquad I_b\dot{\Omega}_b + \Omega_b \times (I_b\Omega_b) = M_t \tag{1}$$

where m is the mass and the I_b is the inertia matrix expressed in the body frame B. The total force F_t acting on the vehicle's center of gravity is the sum of the forces F_{th} created by the rotors, F_w the lift and drag forces generated by the wings, F_g due to gravity, F_d due to external disturbances (e.g. wind, gusts), namely $F_t = F_{th} + F_w + F_g + F_d$ where

$$F_{th} = \begin{bmatrix} c_{\theta_1} & c_{\theta_2} & c_{\theta_3} & c_{\theta_4} \\ 0 & 0 & 0 & 0 \\ -s_{\theta_1} & -s_{\theta_2} & -s_{\theta_3} & -s_{\theta_4} \end{bmatrix} \begin{bmatrix} k{\omega_1}^2 \\ k{\omega_2}^2 \\ k{\omega_3}^2 \\ k{\omega_4}^2 \end{bmatrix}, \; F_w = \begin{bmatrix} (F_D^1(\theta_1, v_x, v_z) + F_D^2(\theta_2, v_x, v_z) + F_D^3(\theta_3, v_x, v_z) + F_D^4(\theta_4, v_x, v_z)) \\ 0 \\ (F_L^1(\theta_1, v_x, v_z) + F_L^2(\theta_2, v_x, v_z) + F_L^3(\theta_3, v_x, v_z) + F_L^4(\theta_4, v_x, v_z)) \end{bmatrix}$$

and $F_g = \begin{bmatrix} -s_\theta & s_\phi c_\theta & c_\phi c_\theta \end{bmatrix}^T mg$, where s_β and c_β are abbreviations for $\sin(\beta)$ and $\cos(\beta)$ respectively. Note that the propeller thrusts $F_{(1,2,3,4)}$ are modeled as $F_i = k\omega_i^2$, where ω_i is the propeller's rotational speed.

Because the wings at the back are rotated together, their angle of attacks are the same for all time ($\theta_3 = \theta_4$). Note that the lift forces $F_L^i(\theta_i, v_x, v_z)$ and the drag forces $F_D^i(\theta_i, v_x, v_z)$ are not just functions of linear velocities (v_x and v_z) like on a fixed-wing type of an airplane, but also functions of angle of attack θ_i for each wing, namely $\begin{bmatrix} F_D^i & 0 & F_L^i \end{bmatrix}^T = R(\theta_i) \begin{bmatrix} -\frac{1}{2}c_D(\alpha_i)\rho A v_\alpha^2 & 0 & -\frac{1}{2}c_L(\alpha_i)\rho A v_\alpha^2 \end{bmatrix}^T$ where $v_\alpha = \sqrt{v_x^2 + v_z^2}$ and $\alpha_i = \theta_i - (-atan2(v_z, v_x))$. In these expressions, ρ is the air density, A is the wing area, v_α is the airstream velocity and α_i is the effective angle of attack as shown in Figure 3(a). The $R(\theta_i)$ is the rotation matrix around y axis to transform the lift and drag forces back to the body frame. The lift coefficient $c_L(\alpha_i)$ and drag

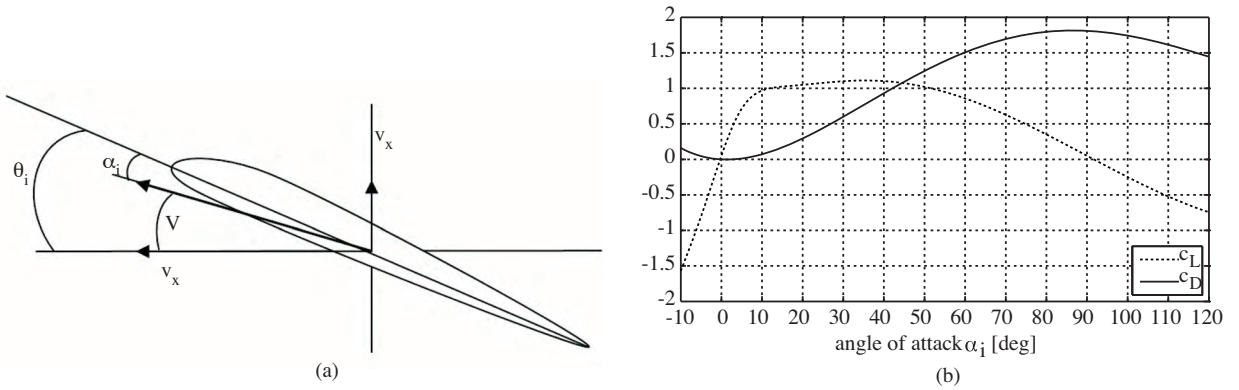

Figure 3. (a) Effective angle of attack α_i, (b) Lift and drag coefficients on large angles of attack.

coefficient $c_D(\alpha_i)$ in Figure 3(b) are modeled according to the data points obtained from Javafoil and airfoil models from [21], [22].

The total torque M_t acting on the vehicle's center of gravity is the sum of the torques M_{th} created by the rotors, M_w created by the drag/lift forces of the wings, M_{gyro} created by the gyroscopic effects of the

propellers and M_d due to external disturbances, namely $M_t = M_{th} + M_w + M_{gyro} + M_d$ where

$$M_{th} = \begin{bmatrix} l_s s_{\theta_1} - c_{\theta_1}\lambda_1 & -l_s s_{\theta_2} - c_{\theta_2}\lambda_2 & l_s s_{\theta_3} - c_{\theta_3}\lambda_3 & -l_s s_{\theta_4} - c_{\theta_4}\lambda_4 \\ l_l s_{\theta_1} & l_l s_{\theta_2} & -l_l s_{\theta_3} & -l_l s_{\theta_4} \\ l_s c_{\theta_1} + s_{\theta_1}\lambda_1 & -l_s c_{\theta_2} + s_{\theta_2}\lambda_2 & l_s c_{\theta_3} + s_{\theta_3}\lambda_3 & -l_s c_{\theta_4} + s_{\theta_4}\lambda_4 \end{bmatrix} \begin{bmatrix} k{\omega_1}^2 \\ k{\omega_2}^2 \\ k{\omega_3}^2 \\ k{\omega_4}^2 \end{bmatrix},$$

$$M_w = \begin{bmatrix} l_s(F_L^1(\theta_1, v_x, v_z) - F_L^2(\theta_2, v_x, v_z)) \\ l_l(F_L^1(\theta_1, v_x, v_z) + F_L^2(\theta_2, v_x, v_z) - F_L^3(\theta_3, v_x, v_z) - F_L^4(\theta_4, v_x, v_z)) \\ l_s(-F_D^1(\theta_1, v_x, v_z) + F_D^2(\theta_2, v_x, v_z)) \end{bmatrix}, \quad M_{gyro} = \sum_{i=1}^{4} J_p[\eta_i \Omega_b \times \begin{bmatrix} c_{\theta_i} \\ 0 \\ -s_{\theta_i} \end{bmatrix} \omega_i]$$

In the above equations, $\eta_{(1,2,3,4)} = 1, -1, -1, 1$, J_p is the inertia of the propellers about the rotation axis. The propeller torques $T_{(1,2,3,4)}$ are modeled as $T_i = \lambda_i k \omega_i^2$, where $\lambda_{1,2,3,4}$ are torque/force ratios. For clockwise rotating propellers, λ_2, λ_3 are negative whereas λ_1, λ_4 are positive for counterclockwise rotating propellers. It turns out that λ for such kind of propeller sets are measured as 1-5% in the literature [20]. Note that the sum of torques created by the rotors result in a roll moment along the x axis in horizontal flight mode ($\theta_{1,2,3,4} = 0$) and in a yaw moment along the z axis in vertical flight mode ($\theta_{1,2,3,4} = \pi/2$).

3. Vertical flight controllers design

To synthesize various controllers, equations derived in Section 2 are rewritten in state-space form as

$$\dot{\chi} = \begin{bmatrix} \dot{P}_w \\ \dot{V}_b \\ \dot{\Omega}_b \\ \dot{\alpha_w} \end{bmatrix} = \begin{bmatrix} R^{-1}(\alpha_w) \cdot V_b \\ 1/m \cdot [F_t - \Omega_b \times (m \cdot V_b)] \\ I_b^{-1} \cdot [M_t - \Omega_b \times (I_b \cdot \Omega_b)] \\ E^{-1}(\alpha_w) \cdot \Omega_b \end{bmatrix} = f(\chi, u) \tag{2}$$

where the state vector χ consists of the position (P_w), the attitude (α_w), the linear velocity (V_b) and the angular velocity (Ω_b), i.e. $\chi = \begin{bmatrix} P_w & V_b & \Omega_b & \alpha_w \end{bmatrix}^T$. When the aerial vehicle is in vertical flight mode (i.e. $\theta_{1,2,3,4} = \pi/2$), the nonlinear dynamics boil down to the dynamics of a quadrotor given by

$$\dot{V}_b = \begin{bmatrix} -g s_\theta + r v_y - q v_z \\ g s_\phi c_\theta - r v_x + p v_z \\ \frac{-k}{m}(\omega_1^2 + \omega_2^2 + \omega_3^2 + \omega_4^2) + g c_\theta c_\phi + q v_x - p v_y \end{bmatrix}, \quad \dot{\Omega}_b = \begin{bmatrix} \frac{l_s k(\omega_1^2 - \omega_2^2 + \omega_3^2 - \omega_4^2) + J_p(-\omega_1 + \omega_2 + \omega_3 - \omega_4)q + (I_{yy} - I_{zz})rq}{I_{xx}} \\ \frac{l_l k(\omega_1^2 + \omega_2^2 - \omega_3^2 - \omega_4^2) + J_p(\omega_1 - \omega_2 - \omega_3 + \omega_4)p + (I_{zz} - I_{xx})pr}{I_{yy}} \\ \frac{k(\lambda_1\omega_1^2 + \lambda_2\omega_2^2 + \lambda_3\omega_3^2 + \lambda_4\omega_4^2) + (I_{xx} - I_{yy})pq}{I_{zz}} \end{bmatrix} \tag{3}$$

where I_{xx}, I_{yy} and I_{zz} are the inertias of the vehicle around x, y, z axes.

The parameters used in the dynamic model of the vehicle are given in Table 1 where COG denotes the center of gravity of the vehicle.

The total propeller speed is defined as $\omega_p \triangleq \omega_1 - \omega_2 - \omega_3 + \omega_4$. Let us also define the following four virtual control inputs (u_i) in terms of actuating forces and torques as

$$u = \begin{bmatrix} u_1 \\ u_2 \\ u_3 \\ u_4 \end{bmatrix} = \begin{bmatrix} -k\ (\omega_1^2 + \omega_2^2 + \omega_3^2 + \omega_4^2) \\ k\ l_s(\omega_1^2 - \omega_2^2 + \omega_3^2 - \omega_4^2) \\ k\ l_l(\omega_1^2 + \omega_2^2 - \omega_3^2 - \omega_4^2) \\ k\ (\lambda_1\omega_1^2 + \lambda_2\omega_2^2 + \lambda_3\omega_3^2 + \lambda_4\omega_4^2) \end{bmatrix} \tag{4}$$

Table 1. Modeling parameters.

Symbol	Description	Magnitude
m	mass	4 kg
l_s	rotor distance to COG along y axis	0.25 m
l_l	rotor distance to COG along x axis	0.25 m
I_{xx}	moment of inertia	0.195 kgm^2
I_{yy}	moment of inertia	0.135 kgm^2
I_{zz}	moment of inertia	0.135 kgm^2
$\lambda_{1,4}$	torque/force ratio	0.01 Nm/N
$\lambda_{2,3}$	torque/force ratio	-0.01 Nm/N

With these definitions, Equation (3) can be simplified to

$$\dot{V}_b = \begin{bmatrix} \dot{v}_x \\ \dot{v}_y \\ \dot{v}_z \end{bmatrix} = \begin{bmatrix} -gs_\theta + rv_y - qv_z \\ gs_\phi c_\theta - rv_x + pv_z \\ \frac{u_1}{m} + gc_\theta c_\phi + qv_x - pv_y \end{bmatrix}, \quad \dot{\Omega}_b = \begin{bmatrix} \dot{p} \\ \dot{q} \\ \dot{r} \end{bmatrix} = \begin{bmatrix} \frac{u_2}{I_{xx}} + \frac{J_p}{I_{xx}}\omega_p q + \frac{I_{yy}-I_{zz}}{I_{xx}}qr \\ \frac{u_3}{I_{yy}} + \frac{J_p}{I_{yy}}\omega_p p + \frac{I_{zz}-I_{xx}}{I_{yy}}pr \\ \frac{u_4}{I_{zz}} + \frac{I_{xx}-I_{yy}}{I_{zz}}pq \end{bmatrix} \tag{5}$$

Note that these equations are expressed in body frame. For attitude or orientation control, the last three equations will be directly employed in control formulation. For altitude control, on the other hand, we need to express the third component of $\dot{V}_b$, i.e. Z dynamics, in earth frame. To this end, we use the orientation matrix between the body and the earth frames and obtain the following altitude dynamics:

$$\ddot{Z} = (c_\phi c_\theta)\frac{u_1}{m} + g \tag{6}$$

Altitude and attitude dynamics can be linearized around hover conditions, i.e. $\phi \approx 0$, $\theta \approx 0$ and $\psi \approx 0$, where angular accelerations in body and world frames can be assumed to be approximately equal, i.e. $\dot{p} \approx \ddot{\phi}$, $\dot{q} \approx \ddot{\theta}$, $\dot{r} \approx \ddot{\psi}$. Resulting linearized altitude and attitude dynamics can be expressed in earth frame W as

$$\ddot{Z} = \frac{u_1}{m} + g, \quad \ddot{\phi} = \frac{u_2}{I_{xx}}, \quad \ddot{\theta} = \frac{u_3}{I_{yy}}, \quad \ddot{\psi} = \frac{u_4}{I_{zz}} \tag{7}$$

3.1. Altitude and attitude stabilization using PID controllers

A gravity compensated PID controller is designed for altitude control. For attitude control, three classical PID controllers are designed to stabilize the vehicle in hover mode. Controllers designed for the altitude, roll, pitch and yaw are given by the following equations:

$$u_1 = m(-g + K_{p,z}e_z + K_{d,z}\dot{z} + K_{i,z}\int e_z)$$

$$u_2 = I_{xx}(K_{p,\phi}e_\phi + K_{d,\phi}\dot{\phi} + K_{i,\phi}\int e_\phi)$$

$$u_3 = I_{yy}(K_{p,\theta}e_\theta + K_{d,\theta}\dot{\theta} + K_{i,\theta}\int e_\theta)$$

$$u_4 = I_{zz}(K_{p,\psi}e_\psi + K_{d,\psi}\dot{\psi} + K_{i,\psi}\int e_\psi) \tag{8}$$

where $e_q = q^d - q$ for $q = Z, \phi, \theta, \psi$. In these controllers $K_{p,q} > 0$, $K_{d,q} > 0$ and $K_{i,q} > 0$ are proportional, derivative and integral control gains, respectively.

4. Experimental results

PID controllers designed in the previous section are implemented in onboard microprocessor of the vehicle and experimentally tested in both indoor and outdoor environments. In Figure 4, flight scenes from indoor and outdoor hovering experiments of SUAVI are shown.

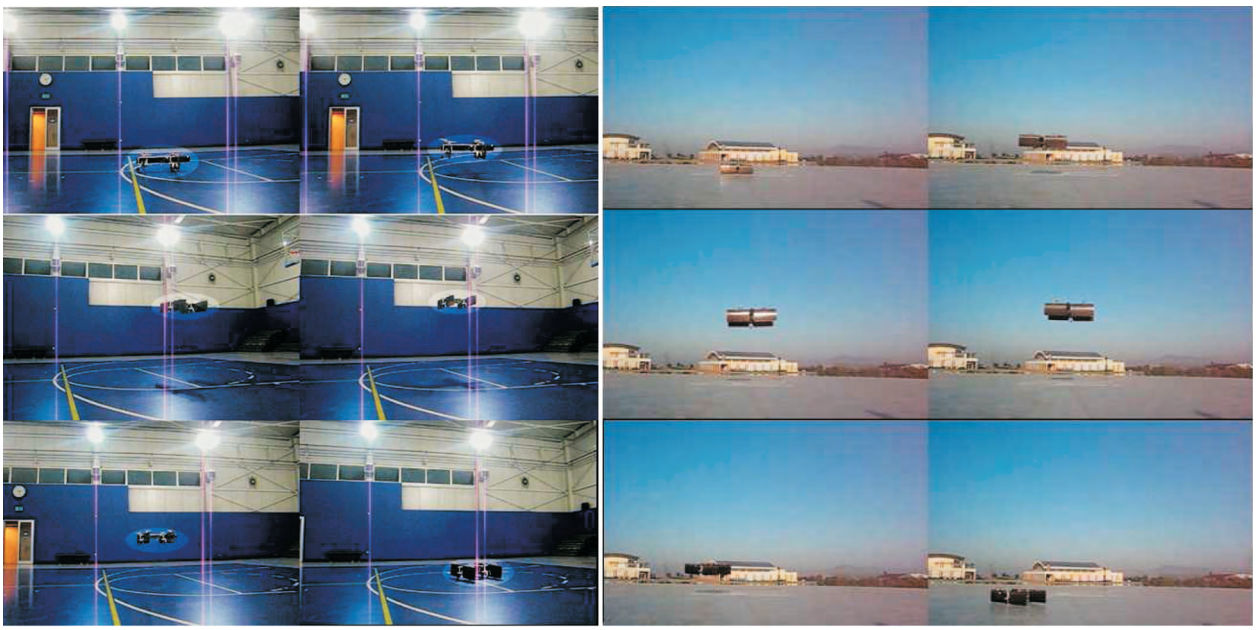

(a) (b)

Figure 4. Indoor (a) and outdoor (b) flight experiments.

Satisfactory attitude control performance is obtained by PID controller as shown in outdoor flight test depicted in Figure 5(a). Attitude references given by a pilot are tracked with very small errors $(2^\circ - 3^\circ)$. Notice that the responses of the PD controllers are fast enough to enable robust roll and pitch stabilization. Similarly, the experimental result related to the designed altitude controller is given in Figure 5(b). The vehicle is kept at the desired altitude successfully where a maximum of 30 cm tracking error occurs as an overshoot in the transient response.

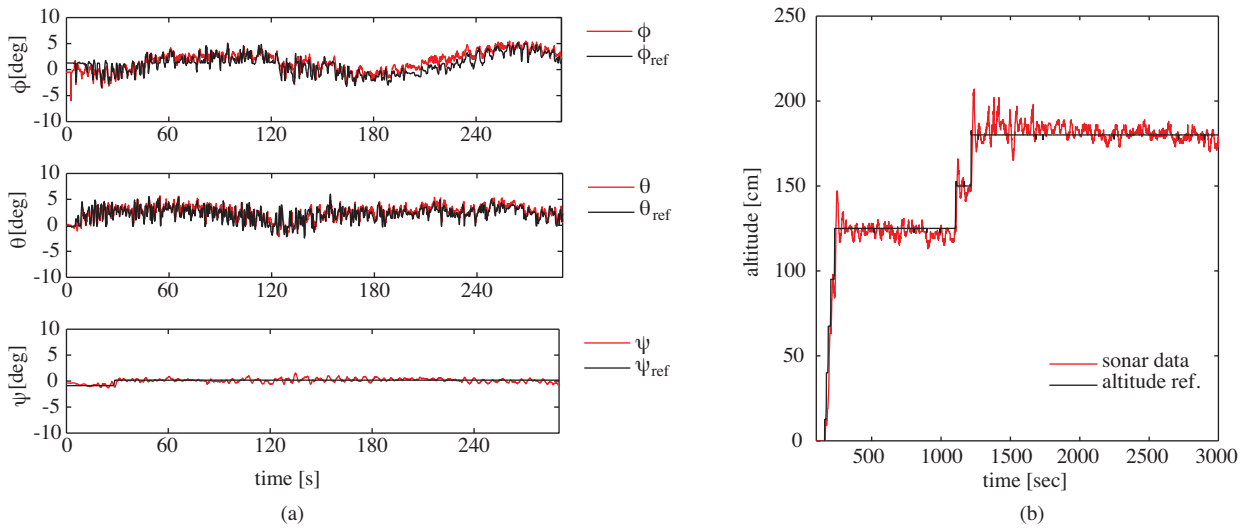

Figure 5. Outdoor flight test: attitude stabilization using PID (a), altitude control using gravity compensated PID (b).

5. Conclusion and future works

The full mathematical model of the tilt-wing aerial vehicle is derived using Newton-Euler formulation. A gravity compensated PID controller is designed and implemented for altitude control. PID controllers are designed and implemented for attitude stabilization. Performances of the proposed controllers are very good as demonstrated by sufficiently small altitude and attitude errors obtained from indoor and outdoor flight experiments.

Future works include design and implementation of position control and trajectory tracking algorithms on our aerial vehicle SUAVI.

Acknowledgements

Authors would like to acknowledge the support provided by TUBITAK under grant 107M179.

References

[1] G. Klein, B. Roberts, and C. Seymour, "MV-22 Handling Qualities Flight Test Summary," American Helicopter Society 56th Annual Forum, Virginia Beach, VA, May 2000.

[2] The Bell Eagle Eye UAS, (2008, September 13). http://www.bellhelicopter.com/en/aircraft/military/bellEagleEye.cfm

[3] J. J. Dickeson, D. Miles, O. Cifdaloz, Wells, V.L. Rodriguez, A.A., "Robust LPV H Gain-Scheduled Hover-to-Cruise Conversion for a Tilt-Wing Rotorcraft in the Presence of CG Variations," *ACC '07*, pp.5266-5271, 9-13 July 2007

[4] F. Kendoul, I. Fantoni, R. Lozano, "Modeling and control of a small autonomous aircraft having two tilting rotors," *Proceedings of the 44th IEEE Conference on Decision and Control*, December 12-15, Seville, Spain, 2005

[5] D. Snyder, "The Quad Tiltrotor: Its Beginning and Evolution," Proceedings of the 56th Annual Forum, *American Helicopter Society*, Virginia Beach, Virginia, May 2000.

[6] K. Nonami, "Prospect and Recent Research & Development for Civil Use Autonomous Unmanned Aircraft as UAV and MAV," *Journal of System Design and Dynamics*, Vol.1, No.2, 2007

[7] S. Bouabdallah, A. Noth and R. Siegwart, "PID vs LQ Control Techniques Applied to an Indoor Micro Quadrotor," *Proc. of 2004 IEEE/RSJ Int. Conference on Intelligent Robots and Systems*, September 28 - October 2, Sendai, Japan, 2004.

[8] B. Erginer and E. Altug, "Modeling and PD control of a Quadrotor VTOL Vehicle," *Proc. of the 2007 IEEE Intelligent Vehicles Symposium*, June 13-15 Istanbul, Turkey, 2007.

[9] A. Tayebi and S. McGilvray, "Attitude Stabilization of a Four-Rotor Aerial Robot," *43rd IEEE Conference on Decision and Control*, December 14-17 Atlantis, Paradise Island, Bahamas, 2004.

[10] H. Voos, "Nonlinear State-Dependent Riccati Equation Control of a Quadrotor UAV," *Proc. of the 2006 IEEE Int. Conference on Control Applications* Oct 4-6, Munich, Germany, 2006.

[11] J. Lee, O. Purwin, and R.D'Andrea, "Design and control of a four-rotor autonomous flying vehicle," *IEEE International Conference on Robotics and Automation*, May, 2006

[12] M. G. Earl and R. D'Andrea, "Real-time Attitude Estimation Techniques Applied to a Four Rotor Helicopter," *43rd IEEE Conference on Decision and Control*, December 14-17 Atlantis, Paradise Island, Bahamas, 2004.

[13] D. Lee, T. C. Burg, B. Xian and D. M. Dawson, "Output Feedback Tracking Control of an Underactuated Quad-Rotor UAV" *Proc. of the 2007 American Control Conference*, July 11-13 New York City, USA, 2007.

[14] T. Madani and A. Benallegue, "Backstepping Control with Exact 2-Sliding Mode Estimation for a Quadrotor Unmanned Aerial Vehicle," *Proc. of the 2007 IEEE/RSJ Int. Conf. IROS*, Oct 29 - Nov 2, San Diego, CA, USA, 2007

[15] S. L. Waslander, G. M. Hoffmann, J. S. Jang and C. J. Tomlin, "Multi-Agent Quadrotor Testbed Control Design: Integral Sliding Mode vs Reinforcement Learning," *Proc. of the 2005 IEEE/RSJ Int. Conf. IROS*, 2005

[16] T. Cheviron, A. Chriette, F. Plestan, "Generic Nonlinear Model of Reduced Scale UAVs," *Proceedings of the IEEE ICRA*, Kobe, Japan, May 12-17 2009

[17] A. Hably and N. Merchand, "Global stabilization of a four rotor helicopter with bounded inputs," *Proc. of the 2007 IEEE/RSJ Int. Conference on Intelligent Robots and Systems*, Oct 29 - Nov 2, San Diego, CA, USA, 2007

[18] S. Leven, J. Zufferey, D. Floreano "A Minimalist Control Strategy for Small UAVs," *Proceedings of the IEEE International Conference on Intelligent Robots and System*, St. Luis, USA, October 11-15 2009

[19] H. Huang, G. M. Hoffman, S. L. Waslander, C. J. Tomlin "Aerodynamics and Control of Autonomous Quadrotor Helicopters in Aggressive Maneuvering," *Proceedings of the IEEE ICRA*, Kobe, Japan, May 12-17 2009

[20] T. Bresciani, "Modeling Identification and Control of a Quadrotor Helicopter," *Master Thesis, Department of Automatic Control, Lund University*, October, 2008.

[21] I. H. Abbott and A. E. von. Doenhoff, Theory of Wing Sections, *Dover Publications Inc.*, 1959

[22] R. E. Sheldahl and P. C. Klimas, "Aerodynamic Characteristics of Seven Symmetrical Airfoil Sections Through 180 Degree Angle of Attack For Use in Aerodynamic Analysis of Vertical Axis Wind Turbines," *Sandia National Laboratories Report SAND80-2114*, July, 1981